Atomic Mutations at the Single Tryptophan Residue of Human Recombinant Annexin V: Effects on Structure, Stability, and Activity‡

Caroline Minks,* Robert Huber, Luis Moroder, and Nediljko Budisa*

Max-Planck-Institut für Biochemie, D-82152 Martinsried, Germany

Received March 12, 1999; Revised Manuscript Received May 3, 1999

ABSTRACT: The single tryptophan residue (Trp187) of human recombinant annexin V, containing 320 residues and 5328 atoms, was replaced with three different isosteric analogues where hydrogen atoms at positions 4, 5, and 6 in the indole ring were exchanged with fluorine. Such single atom exchanges of H → F represent atomic mutations that result in slightly increased covalent bond lengths and inverted polarities in the residue side-chain structure. These minimal changes in the local geometry do not affect the secondary and tertiary structures of the mutants, which were identical to those of wild-type protein in the crystal form. But the mutants exhibit significant differences in stability, folding cooperativity, biological activity, and fluorescence properties if compared to the wild-type protein. These rather large global effects, resulting from the minimal local changes, have to be attributed either to the relatively strong changes in polar interactions of the indole ring or to differences in the van der Waals radii or to a combination of both facts. The changes in local geometry that are below resolution of protein X-ray crystallographic studies are probably of secondary importance in comparison to the strong electronegativity introduced by the fluorine atom. Correspondingly, these types of mutations provide an interesting approach to study cooperative functions of integrated residues and modulation of particular physicochemical properties, in the present case of electronegativity, in a uniquely structured and hierarchically organized protein molecule.

Proteins are large heteropolymeric molecules that are cooperatively folded into compact and specific conformations, optimized and highly specialized for specific biological tasks via precise three-dimensional arrangements of functional groups. Apart from posttranslational modifications, the functional diversification of proteins can also be achieved by expanding the pool of amino acids cotranslationally introduced into proteins in vivo (*1*). The goal is to minimize as much as possible deleterious effects on structure and function and, if possible, to insert probes of intrinsically new properties such as new spectral windows that differ from the native one (*2*). The amino acid tryptophan is an attractive target for such studies for at least two reasons: (i) its low abundance in proteins (in average one residue per protein) and (ii) its dominant intrinsic chromophoric properties which are strongly affected by its local environment, e.g., fluorescence emission spectrum and quantum yields. The tryptophan-related properties of proteins, e.g., the fluorescence, are specific and a kind of fingerprint of the protein structure (*3*).

The first experiments of bioincorporation of tryptophan-like noncanonical amino acids were performed in the 1950s and 1960s (*4*−*6*). However, only the advent of recombinant DNA technology made it possible to establish reliable, simple and easily reproducible in vivo protocols for efficient protein labeling in particular auxotrophic expression hosts (*1, 7, 8*). In the past fluorinated aromatic amino acids were often successfully used for ^{19}F NMR studies on ^{19}F-labeled proteins, facilitating chemical shift calculations (*9*). On the other hand, it is well established that fluorinated tryptophans can provide unique spectroscopic properties when introduced into proteins. For example, 4-fluorotryptophan as a nonfluorescent analogue allows for identification of spectroscopic contributions of "hidden" chromophores such as tyrosines or phenylalanines in proteins (*10*), providing a sophisticated tool for protein−protein or protein−DNA interaction studies. Despite these promising aspects, only very recently more systematic analytical as well as biophysical studies of per substituted proteins were reported (*11, 12*).

In the present study we have extended this approach to structural and functional studies of human recombinant annexin V (*13*) as the model protein. Three noncanonical Trp[1] analogues have been inserted into human recombinant annexin V: 4-FTrp, 5-FTrp, and 6-FTrp (Scheme 1). Native as well as mutant proteins were expressed under the control of T7 promoter in the T7 promoter/polymerase system (*14*) using the selective pressure incorporation (SPI) method as described previously (*15*). Annexin V is an ideal model for these types of studies for at least two reasons: (i) there is only one single Trp residue in the molecule, i.e., Trp187, and (ii) this single Trp residue is playing a crucial role for

‡ Structures 6Fav and 5Fav reported in this paper have been deposited in the Protein Data Bank, Biology Department, Brookhaven National Laboratory, Upton, NY 11973.

* Corresponding authors. Tel: 0049 89 8578 2661/2683. Fax: 0049 89 8578 3516. E-mail: budisa@biochem.mpg.de; minks@biochem.mpg.de.

[1] Abbreviations: Trp, tryptophan; 4F-Trp, 4-fluorotryptophan; 5-FTrp, 5-fluorotryptophan, 6-FTrp, 6-fluorotryptophan; SPI, selective pressure incorporation; NMM, new minimal medium; PBS, phosphate-buffered saline; SDS−PAGE, sodium dodecyl sulfate−polyacrylamide gel electrophoresis.

10.1021/bi990580g CCC: $18.00
Published on Web 07/29/1999

Scheme 1: Tryptophan and Its Noncanonical Counterparts Incorporated into Annexin V[a]

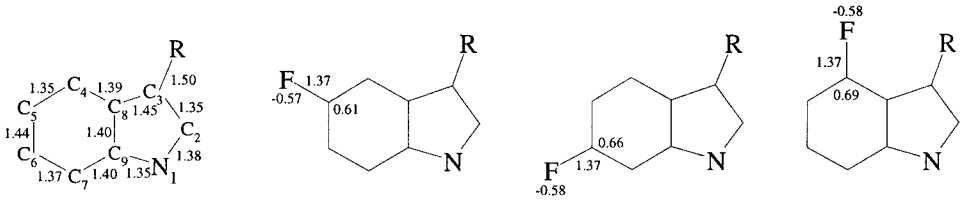

[a] From left to right: tryptophan, 5-fluorotryptophan, 6-fluorotryptophan, and 4-fluorotryptophan. The values for bond lengths (in Å) and net charges are taken from ref *39*.

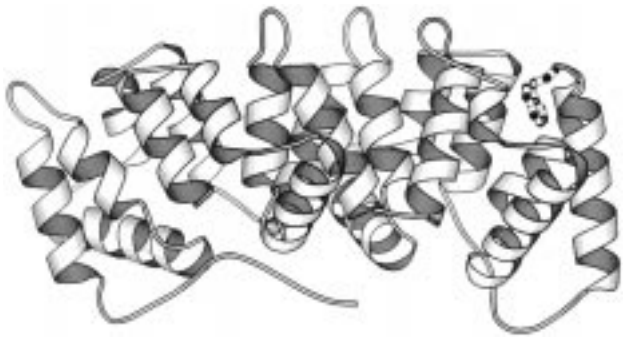

FIGURE 1: Side view of the three-dimensional structure of human recombinant annexin V represented as a ribbon plot using the program MOLSCRIPT (*48*). Residue Trp187 (shown in ball-and-stick representation) is buried in the hydrophobic pocket at the convex side of the molecule.

the Ca^{2+}-dependent membrane binding and related channel activity (*16*). At low calcium concentrations the Trp187-containing loop between helices IIIA and IIIB is buried in a hydrophobic niche (Figure 1) at the convex surface of the protein molecule (*13*), while it exposed to the solvent upon addition of calcium, creating a new calcium-binding site that mediates binding to the membrane (*17*). Fluorescence studies indicate that the tryptophan is particularly inserted into the membrane and in close proximity to the phospholipid headgroups (*16*). Additionally, in the native state of the protein Trp187 is inserted into a hydrophobic pocket making it very suitable for folding and stability studies, since upon denaturant action it undergoes a similar transition to the solvent milieu. Therefore single H → F exchanges were used to study the global effect of these mutations at a defined locus of the annexin V structure (Figure 1) on the folding cooperativity and stability properties of this protein.

MATERIALS AND METHODS

Chemicals and Bacterial Strains

Fluorinated tryptophans (4F-Trp, 5-FTrp, and 6-FTrp) were from Sigma and FURA-2 pentasodium salt was from Calbiochem (San Diego, CA). All other chemicals were purchased from Sigma or Aldrich unless stated otherwise. For biosynthetic incorporation the tryptophan-deficient *Escherichia coli* strains from ATCC (catalog numbers 49979, and 49980, respectively) were used. In addition, initial expression experiments were performed using *E. coli W3110 trpR tna2 trpEA2* ("KK8") that lacks the entire trp operon and has nonreverting lesions in the trytophanase gene (*tna*). This strain was a generous gift from Prof. Kasper Kirschner (Biozentrum der Universität Basel, Switzerland).

Expression and Purification of Fluorotryptophan Mutants

Trp auxotrophic E. coli ATCC 49980 (WP2) was used for all expression experiments. The cells were transformed with two plasmids: ampicillin-resistant pRSET-PP4 (*14*) harboring the annexin V gene sequence under the control of T7 promoter and kanamycin-resistant pGP1-2 containing a gene for T7 polymerase (*18*). Cultures were grown under the selective pressure of 100 mg/L ampicillin and 70 mg/L kanamycin. All growth experiments were performed in new minimal medium (NMM) (*19*). Bacterial growth and expression experiments were performed exactly as described previously (*20*).

Protein Purification and Yields. The purification procedures for the expressed mutants of human recombinant annexin V were identical to those of the wild-type protein (*14*). The purity of the proteins was analyzed by SDS−PAGE (silver staining), HPLC, and electrospray mass analysis. As described elsewhere, the SPI method allows for expression of mutants in yields often similar to those of the wt protein form (*15*). For example, with 4-FTrp expression and protein yields were as good as for wt annexin V (20−30 mg/L of culture) using the strain *E. coli* ATCC 49980. Protein yields for the 6-FTrp and 5-FTrp annexin V mutants were always lower (about 15 mg/L of medium) than those of the wt protein.

Analytical Methods

Mass Spectrometric Analysis. The quantitative replacement of the native tryptophan residue by the fluorinated noncanonical analogues was routinely confirmed by electrospray mass spectrometric analyses (ESI-MS) as described elsewhere (*14*).

Amino Acid Analysis. Protein probes of approximately 10 nM were hydrolyzed in 6 M HCl containing 2.5% (v/v) thioglycolic acid for 48 h. The hydrolysates were analyzed with a Biotronic LC 6001 amino acid analyzer. The fluorinated Trp analogues were subjected to hydrolysis under identical conditions to determine both retention times and recoveries. Only 5-FTrp was found to elute under standard conditions and was used to identify this residue in the 5-FTrp mutant, whereas for the other mutants the absence of Trp in the hydrolysate was used as the index for quantitative Trp replacement by the fluorinated analogues.

Structural Analysis by Spectroscopy

Fluorescence. Fluorescence spectra were recorded on a Perkin-Elmer luminescence spectrometer (LS50B) equipped with digital software. Samples of proteins were prepared at 2 μM concentration in PBS (phosphate-buffered saline) or 10 mM Tris-HCl (pH 8.0) and were excited at 280 nm (slit

Table 1: Data Collection and Refinement Parameters

5-FTrp annexin V		6-FTrp annexin V	
space group	*R*3	space group	*R*3
cell constants (Å)	$a = b = 99.73$, $c = 97.14$	cell constants (Å)	$a = b = 99.83$, $c = 97.04$
limiting resolution (Å)	2.7	limiting resolution (Å)	2.3
reflections unique	8543	reflections unique	15967
completeness (%)		completeness (%)	
overall (19.0−2.50)	92.4	overall (19.0−2.50)	96.3
last shell (2.82−2.7)	99.4	last shell (2.41−2.30)	95.8
R_{merge}[a] (%)	8.5	R_{merge}[a] (%)	6.2
molecules per asym unit	1	molecules per asym unit	1
resolution range (Å)	19−2.7	resolution range (Å)	19−2.3
crystallographic R-factor[b] (%)	21.1	crystallographic R-factor[b] (%)	22.4
free *R*-factor[c] (%)	25.8	free *R*-factor[c] (%)	26.8
rms deviations		rms deviations	
bond lengths (Å)	2.041	bond lengths (Å)	1.083
bond angles (deg)	0.015	bond angles (deg)	0.005
no. of non-hydrogen atoms	2497	no. of non-hydrogen atoms	2497
solvent molecules	121	solvent molecules	101

[a] $R_{merge} = \sigma[I(h)_i - \langle I(h)\rangle]/\sigma\langle I(h)\rangle$; $I(h)_i$ is the observed intensity of the *i*th measurement of reflection *h*, and $I(h)$ is the mean intensity of reflection *h* calculated after loading and scaling. [b] *R*-factor $= \sigma[|F_o| - |F_c|]/|F_o| \times 100$. [c] R_{free} was calculated randomly, omitting 10% of the observed reflections from refinement and *R*-factor calculation.

2.5) and 295 nm, respectively, and the emission spectra were recorded in the 310−500 nm range.

Circular Dichroism. The far-UV CD spectra were recorded on a dichrograph Mark IV from Jobin Yvon (Longjumaeu, France) equipped with a thermostated cell holder and connected to a data station for signal averaging and processing. For secondary structure determination spectra were taken in the 195−250 nm wavelength range. These spectra are averages of three scans and are reported as mean residue ellipticity ($[\theta]_R$) in deg cm^2 dmol^{-1}. Protein concentrations of 0.08 mg/mL in PBS containing 10% glycerol were used, and the spectra were measured in quartz cells of 0.1 cm optical path length. Near-UV CD spectra in the aromatic region (250−350 nm) were recorded at protein concentrations of 0.5 mg/mL in Tris-HCl (pH 8.0). To obtain sufficient dichroic intensity, 10 scans were accumulated per spectrum, and the resulting values are averaged and expressed as molar ellipticity ($[\theta]_M$).

Melting Curves. CD melting curves were determined by monitoring the changes in the dichroic intensity at 222 nm as a function of temperature. For thermal denaturation experiments in a range from 10 to 80 °C, a heating rate of 0.5 °C/min was applied by a Lauda RKS thermostat, using an oil-jacketed cylindrical cell (Hellma, Forest Hills, NY).

Thermodynamic Parameters. The midpoint of denaturation (melting temperature or T_m value) as well as the van't Hoff enthalpy (ΔH_m) was determined using essentially the same methods reported previously (*20*).

Bioactivity. Artificial liposomes containing the calcium-sensitive dye FURA-2 were used to monitor annexin V induced calcium influx (*21*). Vesicle preparations and calcium influx assay for native and substituted proteins were performed as described previously (*21, 22*).

X-ray Crystallographic Analysis

Fluorine-containing annexin V mutants were dialyzed against 10 mM Tris-HCl buffer (pH 8.5) and concentrated to 8−10 mg/mL. To 10 μL of protein solution were added 1 μL of 20 mM $CaCl_2$ solution and 1.5 μL of 2.0 M buffered ammonium sulfate precipitant. Crystallization was achieved at room temperature by vapor diffusion against 2.0 M ammonium sulfate buffered with 0.1 M Tris-HCl (pH 8.5). In all cases the rhombohedral crystals grew after 4−5 days and were harvested into 3 M ammonium sulfate, 0.1 M Tris-HCl (pH 8.5), and 1 mM $CaCl_2$. Their space group is *R*3 with the lattice constants $a = b = 99.73$ Å, $c = 97.14$ Å, $\alpha = \beta = 90°$, and $\gamma = 120°$ (5-FTrp mutant) and $a = b = 99.83$ Å, $c = 97.04$ $\alpha = \beta = 90°$, and $\gamma = 120°$ (6-FTrp mutant) (Table 1). The asymmetric unit contains one molecule (*23*). Diffraction data were collected on an X-ray imaging plate system (Mar Research, Hamburg, Germany) in a thermostated room at 18 °C using Cu Kα radiation from a Rigaku rotating anode generator operated at 5.4 kW to a resolution of 2.7 Å (5-FTrp mutant) and 2.3 Å (6-FTrp mutant). The 4-FTrp annexin V mutant did not crystallize under the conditions described above, as precipitation occurred immediately in the hanging drop.

Reflections were integrated with the program MOSFLM 551 (*24*), scaled and reduced using SALEPACK (*25*) of the CCP4 package (*26*). Crystallographic calculations were mostly performed with X-PLOR (*27*). The atom replacements were determined by the difference Fourier method. Difference maps were inspected on a computer graphic display utilizing the program TURBO−FRODO (*28*).

Molecular Modeling

To visualize and estimate the gap regions (i.e., clefts and cavities) of our target residues in their hydrophobic pockets, we have used the program SURFNET (*29*). The gap regions are calculated exclusively for position 187 while the cavities and surface grooves for the rest of the molecule are not estimated. SUFRNET generates gaps between the native Trp187 (and its noncanonical analogues) and the rest of the molecule using the coordinate data from a PDB file, by fitting spheres between all pairs of atoms and computing 3D density maps which are subsequently contoured, defining the surface of the gap region.

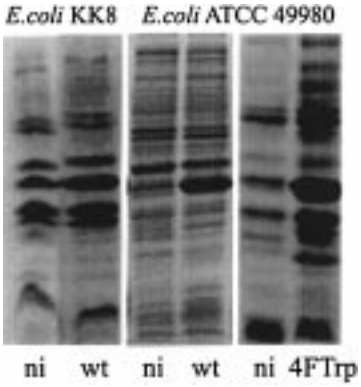

FIGURE 2: Analysis of the recombinant annexin V expression in two different tryptophan auxotrophic *E. coli* strains. Cell lysates from cultures grown in NMM with 0.015 mM Trp as described in the text were prepared by the Laemmli procedure and analyzed in Coomassie blue stained 12% SDS−PA gels (ni, noninduced cell lysates; induced cell lysates are marked as wt and 4-FTrp). *E. coli* strain KK8: note that the level of basal expression (noninduced line) is almost as high as the induced line, making this strain not suitable for quantitative labeling of recombinant proteins. *E. coli* strain ATCC 49980: note that expression in noninduced lines is efficiently suppressed. The induced lines show almost the same level of expression of wild-type AV and 4-FTrp AV as indicated, resulting in a high level of incorporation of the amino acid analogue.

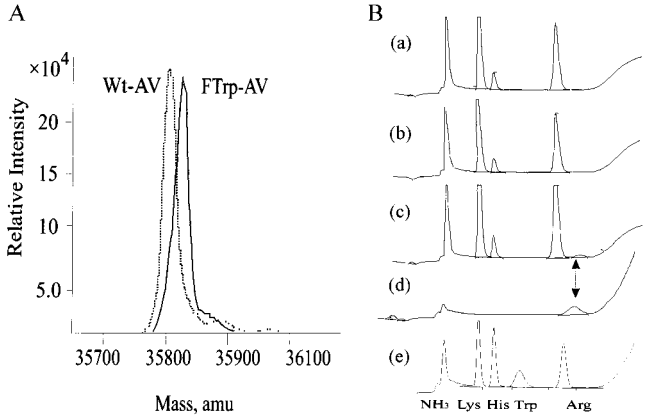

FIGURE 3: Analytical proof for tryptophan analogue incorporation. (A) Mass spectrometric analysis (ESI-MS): Deconvoluted spectra from two separate measurements that are superimposed at the same mass scale. The determined wild-type annexin V mass is 35 809 ± 4 Da as expected, whereas the other peak shows an additional 18 Da in the measured protein (35 827 ± 2.5 Da), indicating successful replacement of Trp187 with 5-FTrp. (b) Portions of the amino acid composition chromatograms for native and analogue containing human recombinant annexin V. Absorbance peaks of ninhydrin derivatives of the amino acids are marked in the standard chromatogram (e). (a) 4-FTrp annexin V. (b) 6-FTrp annexin V. (c) 5-FTrp annexin V; note that 5-FTrp appears in the chromtogram as a peak of very low intensity due to the presence of only one residue in the sequence. (d) The amino acid 5-FTrp alone in the analysis reveals the same retention time as in the protein sample above.

RESULTS

Bioexpression of Fluorotryptophan Mutants by the Selective Pressure Incorporation Method (SPI)

Suitable Expression Hosts. To introduce toxic or even growth-inhibiting noncanonical amino acids by the SPI method in vivo, it is important to use an expression host that (i) exhibits strong and stable auxotrophism, (ii) is suitable for transformation with plasmids and for high level expression of the desired gene product, and (iii) suppresses background expression of the target gene as much as possible. A detailed description of the basic methodological requirements that help to prevent expression of significant quantities of unlabeled protein is described elsewhere (*7*, *14*, *15*, *19*, *20*). In our experimental search for suitable Trp auxotrophic strains (for a useful collection see ref *7*) the main restriction for high-level incorporation of the Trp noncanonical counterparts was the lack of efficient background expression control of the recombinant target gene. Figure 2 illustrates this problem: the *E. coli* strain KK8 exhibits perfect auxotrophism due to the lack of the *trp* operon in the genome, and it is easy to transform with the desired plasmids. However, before induction of protein expression relatively high basal protein synthesis is observed which prevents the possibility of quantitative protein labeling. Conversely, the expression strain ATCC 49980 was found to be much more suitable for labeling recombinant annexin V since it meets all criteria mentioned above (Figure 2).

Toxicity of Fluorotryptophans. Fermentation experiments in the presence of 4-, 5-, and 6-fluorotryptophan clearly show that these fluorinated amino acids inhibit the growth of the strain *E. coli* ATCC 49980 completely. Thus, the cultures were allowed to grow on limiting concentrations of the natural amino acid before addition of the appropriate noncanonical amino acid and induction of the protein synthesis as described elsewhere (*15*).

Optimal Expression Conditions. For the native substrate (Trp) 0.015 mM was found to represent the optimal limiting concentration for the auxotrophic strain *E. coli* ATCC 49980 in NMM (growth stops at an OD_{600} value of about 0.80). This medium provides enough "healthy" cells before depletion of the natural substrate, allowing for the whole culture to reach the mid-logarithmic phase of growth. At this point optimal protein expression and efficient background control are achieved. As shown in Figure 2 expression of the fluoro-Trp containing annexins V is comparable to that of wt annexin V.

Analytical Characterization of the FluoroTryptophan Mutants

Quantitative bioincorporation of 4-, 5-, and 6-FTrp into annexin V was confirmed by amino acid analysis and electrospray mass spectrometry (ESI-MS) coupled with liquid chromatography. In addition, the presence of the fluorine atoms in the indole side chain of Trp187 was fully confirmed by protein X-ray crystallographic and fluorescence profile analyses as discussed below. In fact, the unique fluorescence behavior of 4-FTrp, 5-FTrp, and 6-FTrp allows differentiation these three protein variants.

Fluorinated tryptophans when present in annexin V revealed a mass of 35 827 ± 2.5 Da, which is identical to the expected mass for one H → F replacement at the single Trp187 residue (Figure 3A). Amino acid analysis of the acid hydrolysates performed in the presence of thioglycolic acid allowed detection of Trp for the wt annexin V and 5-FTrp for the 5-FTrp mutant (Figure 3B), whereas 4-FTrp and 6-FTrp are not eluted even by changing the elution conditions to more basic values. However, the complete absence of a Trp peak in the elution profile confirms within the limits of error of this analytical method the quantitative replacement. The different t_R values observed for 5-FTrp and 4- and

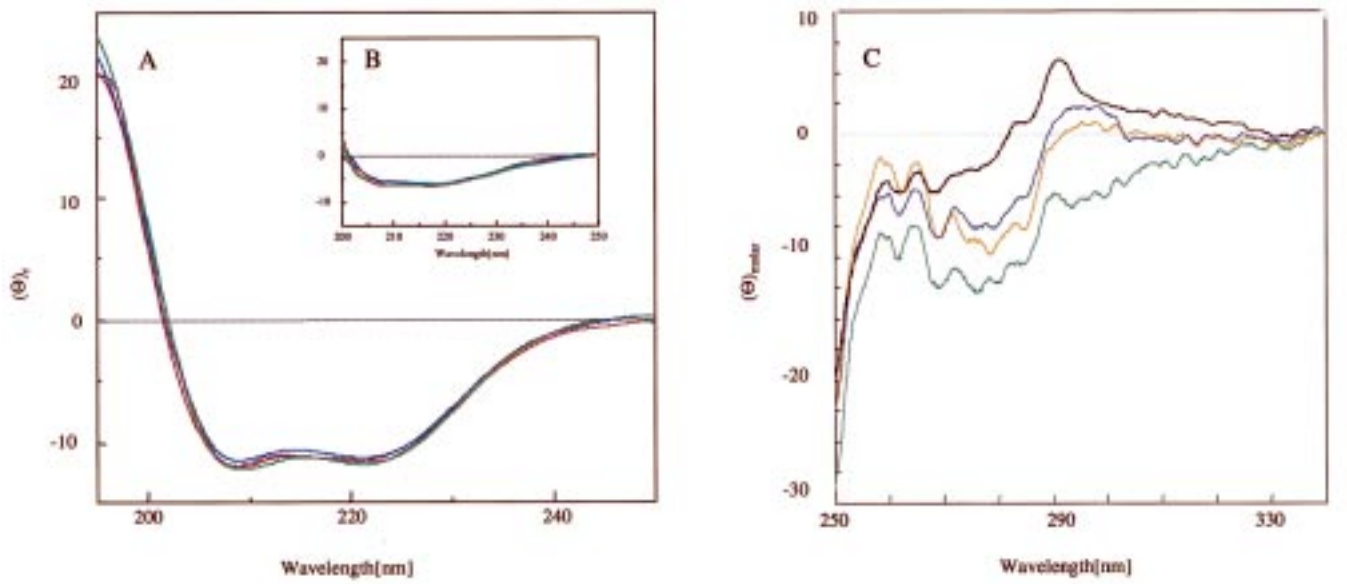

FIGURE 4: Far-UV CD profiles of the native and substituted annexin V protein forms at different temperatures: (black) wt annexin V, (blue) 5-FTrp annexin V, (green) 6-FTrp annexin V, and (red) 4-FTrp annexin V at 10 °C (A) and 80 °C (B). The mean residual ellipticity ($[\theta]_R$) is expressed in deg cm^2 dmol^{-1}. (C) Near-UV CD spectra for wt and mutant annexin V at 25 °C: (black) wt annexin V, (blue) 5-FTrp annexin V, (green) 6-FTrp annexin V, and (red) 4-FTrp annexin V at 25 °C. The mean molar ellipticity ($[\theta]_M$] is expressed in deg cm^2 dmol^{-1}.

6-FTrp would indicate a comparable hydrophobicity of 5-FTrp to that of native Trp and a significantly more hydrophobic character of the two 4- and 6-FTrp analogues.

Conformational Analysis of Annexin V and Its Mutants in Solution

The far-UV CD spectra of wt annexin V and the related mutants in PBS at 10 °C are almost superimposable, thus strongly suggesting identical overall folds at least within the limits of this spectroscopic technique (Figure 4A). Upon heating the solutions to 80 °C (Figure 4B), transition to the denatured state occurred, which is again characterized by similar curve profiles for all mutants. The thermal transition curves show two characteristic features: (a) the isodichroic point near 203 nm for all mutants clearly suggests helix-to-coil transition; (b) the denatured state contains considerable amounts of secondary structure elements that are far from a complete random coil conformation, a phenomenon observed already for other annexin V mutants (*14*) as well as for other proteins such as staphylococcal nuclease (*30*).

The near-UV or aromatic CD spectra of the 4-, 5-, and 6-FTrp mutants are shown in Figure 4C. The characteristics of the spectra of 4-FTrp and 5-FTrp annexin V are very similar to those of the wt protein at pH 7 (*31*). The Phe residues are contributing with a sharp fine structure between 255 and 270 nm and the Tyr residues show a peak between 275 and 282 nm, whereas the Trp dichroism maximum is centered at 290 nm with its fine structure between 290 and 305 nm. All these features can be observed for the different atomic mutants, but the decrease in the intensity of the Trp absorption around 295 nm indicates an increasingly mobile side chain for 4-FTrp and 5-FTrp as well as 6-FTrp as shown in Figure 4. Additionally, for 6-FTrp annexin V a slight blue shift from 295 to 293 nm is observed.

Intrinsic Fluorescence Properties of Annexin V and its Mutants

Native annexin V shows upon excitation at 280 nm a broad emission spectrum in the 318−325 nm range with a maximum centered at 320 nm, while excitation at 295 nm gives emission spectra with maxima at 333 nm (*32*) (Figure 5). Since protein fluorescence and UV absorption are the result of the presence of specific chromophores in the structure, even the intrinsic spectroscopic properties of the particular chromophores of noncanonical amino acid analogues when incorporated into proteins contribute to the overall spectra. Thus, replacement of the single Trp187 with its fluorinated analogues is expected to change the intrinsic spectroscopic properties of annexin V. Bioincorporation of 5-FTrp results in an enhanced quantum yield and a red-shifted emission maximum by about 13 nm to 333 nm (Figure 5A) as previously reported for a 5-FTrp mutant of staphylococcal nuclease (*7*). The 6-FTrp mutant exhibits a similar red shift and enhanced maximum at 336 nm. Conversely, bioincorporation of 4-FTrp into annexin V results in the loss of tryptophan fluorescence, thus revealing mainly the contribution of the Tyr residues to the protein fluorescence emission profile (Figure 5A), which is a general property reported for other proteins as well (*10*). The emission maxima for excitation of the Trp derivatives at 295 nm are shown in Figure 5B, and no fluorescence is detectable for the 4-FTrp annexin V.

Thermal Denaturation

Thermally induced unfolding of wt annexin V occurs as a two-state transition from the α-helical native state to a denatured state (*20*). The denatured state of all the mutants is characterized by significant amounts of secondary structure, as shown in Figure 4B; a more detailed description of the thermodynamic behavior of annexin V was reported previously (*20*).

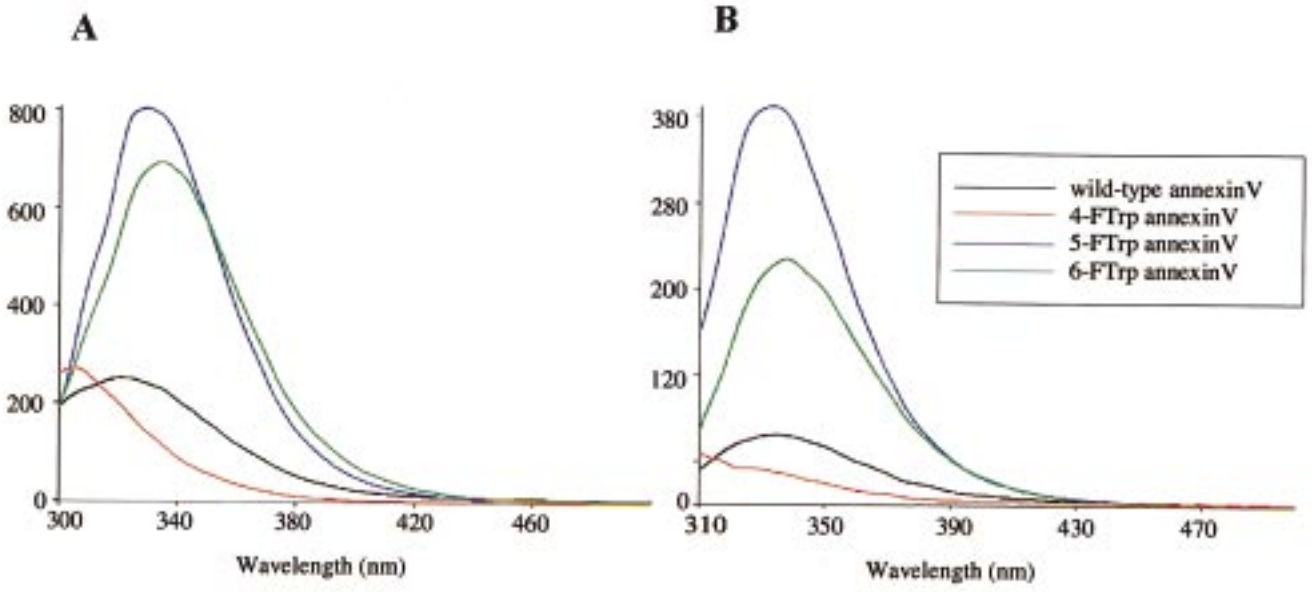

FIGURE 5: Fluorescence emission spectra of (A) native and mutant proteins excited at 280 nm. (B) Excitation at 295 nm. Spectroscopic conditions are described in Materials and Methods.

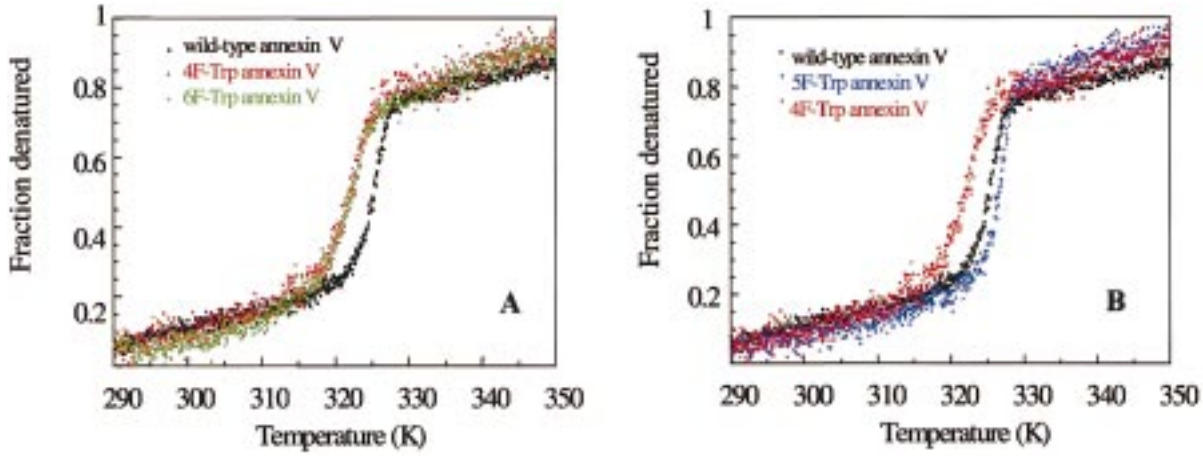

FIGURE 6: Thermal denaturation curves of native and mutant proteins. Fractions of denatured protein are calculated from CD data monitored at 222 nm as described elsewhere (*20*). (A) wt, 4-FTrp, and 6-FTrp annexin. Note that the 4-FTrp and 6-FTrp protein forms exhibit nearly identical denaturation profiles. (B) wt, 4-FTrp, and 5-FTrp annexin. Note that the 5-FTrp-substituted protein has a slightly higher T_m value and a steeper transition part of the denaturing curve. Experimental procedures and calculations for all denaturing curves are described in Materials and Methods.

Table 2: Thermodynamic Parameters of the Denaturation of the Wild-Type and Analogue-Containing Annexin V Mutants[a]

AV mutant	T_m value (K)	ΔT_m	ΔH_m (kJ/mol)
4-FTrp	321.57 ± 0.07	3.3	502.8 ± 18.1
5-FTrp	326.40 ± 0.03	1.5	747.7 ± 15.2
6-FTrp	321.66 ± 0.06	3.2	482.2 ± 13.9
wild type	324.90 ± 0.03		693.3 ± 13.2

[a] Experimental conditions and calculation methods for all unfolding curves are described elsewhere, ΔT_m is the difference between T_m of the native and substituted proteins.

Thermal denaturation was followed by monitoring changes in the dichroic intensities at 222 nm upon heating (Figure 6). For each profile approximately 1000 data points were collected. The thermodynamic parameters derived from the transition curves are reported in Table 2. While the T_m value (324.9 ± 0.089 K) and ΔH_m (693.0 ± 13.3 kJ mol^{-1}) of the wt form coincide with those reported previously (*20*), substitution of the hydrogen atoms at three different positions of a single Trp residue in the annexin V protein molecule leads to values that differ dependent on their position. As already suggested by the near-UV CD spectra, the mutants differ markedly in their thermal stabilities. The denaturation profile of the 5-FTrp atomic mutant shows an increase in the T_m value by 1.5 K while the steeper curve indicates a more cooperative unfolding process (Figure 6B) and consequently a higher (about 8%) estimated ΔH_m value (Table 2). On the other hand, the denaturation profiles for the two other atomic mutants reveal similar T_m values of about 321.6 K, which are 3.3 K lower than that of wt annexin V (Table 2). The ΔH_m values are reduced by about 30% in both atomic mutants with respect to the native protein. This is plausible by taking into account that both curves (Figure 6A) are less steep than that of wt annexin V, indicating a less cooperative unfolding process. Indeed, in our earlier work on methionine atomic mutants we have also observed rather large differences in ΔH_m values that accompany relatively moderate shifts in T_m values. For example, the isosteric replacement

of the sulfur atom (electronegativity 2.58) of the methionine residues with selenium (electronegativity 2.55) in annexin leads to about 25% decrease of the estimated ΔH_m value although the shift in the T_m value is only 1.02 K (*20*).

Biological Activity

Biological activity of annexin V in this study refers to the measurements of the protein-mediated calcium influx and calcium-dependent transition of Trp187.

Calcium-dependent membrane binding of annexin V is assumed to be the first step for ion channel formation through acidic phospholipid bilayers (*22*). To quantify ion channel activities of the annexin V atomic mutants in comparison to the wt protein, FURA-2 assays were performed following essentially the protocol described by Berendes et al. (*21*). The activity factors γ/γ_o [γ/γ_o represents the normalized activity with $\gamma_o = 554 \times 10^{-6}$ arbitrary units (see ref *22*)] derived from these assays for the wt protein and the three mutants were determined according to the method of Hofmann et al. (*22*). The average activity of the native protein was found to be $\gamma/\gamma_o = 25.0$. Unexpectedly, 6-FTrp annexin V is 3 times more active than the wt protein with an average of $\gamma/\gamma_o = 75.3$. On the other hand, the 4-FTrp mutant ($\gamma/\gamma_o = 7.9$) is about 3 times less active and the 5-FTrp mutant ($\gamma/\gamma_o = 12.3$) 2 times less active than the parent protein.

The fluorescence emission maximum of Trp187 is red-shifted upon Ca^{2+} titration and indicates a movement from the hydrophobic core to the solvent (*17*). It corresponds to about 10 nm for wt annexin V, 6 nm for 5-FTrp annexin V, and 4 nm for 6-FTrp annexin V. Due to the "silent fluorescent" properties of 4-FTrp annexin V Ca^{2+} titration experiments could not be performed for this mutant. The Ca^{2+} titration midpoint for the wt protein was reported to be 3 mM (*33*), while in our experiments it amounts to 1.75 $\pm$ 0.20 mM for 5-FTrp and 1.50 $\pm$ 0.15 mM for 6-FTrp annexin V.

X-ray Analysis and Crystal Package Modeling

To explain the surprisingly large differences in the dynamic behavior of the FTrp residues in the related annexin V mutants, crystallization experiments of the protein variants have been performed. While 5-FTrp and 6-FTrp annexin V crystallized under the same conditions as for the wt protein and with nearly identical cell parameters (see Materials and Methods), suitable crystals of the 4-FTrp variant could not be obtained because the protein precipitated. Despite the absence of crystallographic data for the 4-FTrp variant, it is likely that its 3D structure is largely unchanged like the structures of the other two mutants. This is fully supported by far-UV CD data that show almost no difference in secondary structure among the mutants if compared to the wt protein (Figure 4A). On the other hand, the structures of 6-FTrp and 5-FTrp showed almost complete isomorphism concerning their space groups, cell dimensions, and molecules per unit cell. No hydrogen bonding or conformational changes in the neighboring polypeptide chain could be observed, indicating a conserved crystal packing despite the atomic mutations at two different ring positions in the indole moiety and thus their differentiated topochemical environment. Furthermore, a closer inspection of the difference density maps of the structures of the 5-FTrp and 6-FTrp mutants only indicated H $\rightarrow$ F replacements at position 5 and position 6 of the indole ring, respectively (Figure 7).

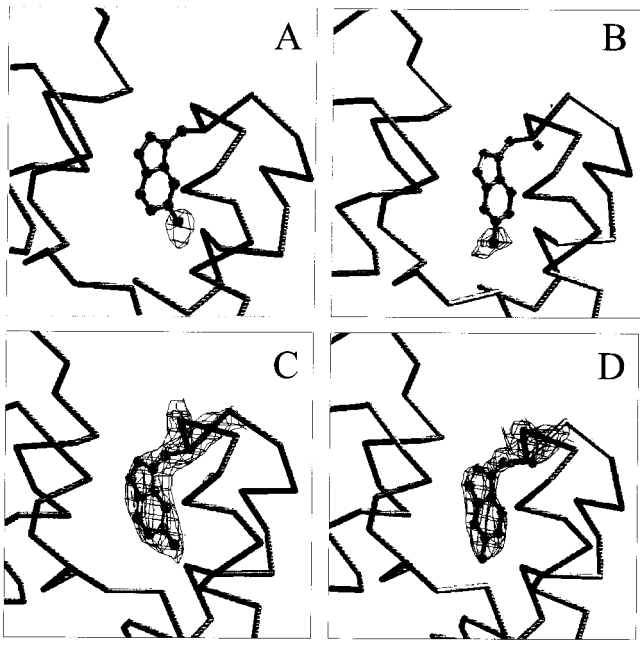

FIGURE 7: Electron density difference ($F_o - F_c$) maps for (A) 6-FTrp 187 and (B) 5-FTrp187 contoured at 3.0 σ. Portions of the continuous electron density maps ($2F_o - F_c$) for (C) 6-FTrp187 (D) 5-FTrp187, both contoured at 1.7σ.

From the X-ray diffraction data a satisfactory explanation for the altered dynamic behavior of the atomic mutants could therefore not be derived. Modeling experiments were performed to estimate the presence of internal cavities and gaps around the Trp187 residue since it is well-known that these could affect protein stability and play an important role in the close packing of amino acid side chains, especially in hydrophobic protein cores (*29*). Figure 8 displays, in the form of blue solid surfaces, the gaps around Trp187 and its analogues as well as the calculated exclusion volumes. It should always be kept in mind that the presented cavity surfaces also correlate with the dynamic behavior of the studied residues. Thus, the resulting data clearly indicate "breathing" of the 4-FTrp and 6-FTrp residues in their local environment to a much larger extent than the Trp residue in the native and 5-FTrp-related mutant structure.

Moreover, the similar shape of the solid surfaces and even the similar values of the exclusion volumes of Trp187 and its 5-FTrp analogue in the proteins indicate a very similar packing into the core, and consequently, these two protein variants should exhibit similar stabilities.

In view of these findings the dynamic behavior of the wt protein and 5-FTrp mutant was expected to be very similar, but different from that of 4-FTrp and 6-FTrp annexin V. Indeed, this was experimentally confirmed by the thermodynamic parameters derived from the thermal transition curves (Figure 6, Table 1). The larger extent of breathing in the case of 4-FTrp and 6-FTrp annexin V reflects a less tightly packed structure, thus leading to lower stabilities.

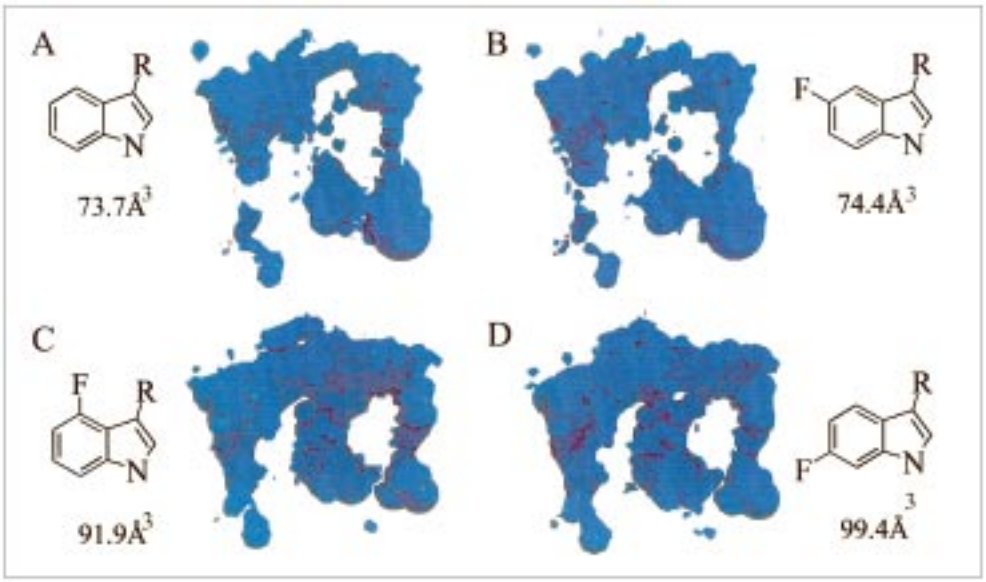

FIGURE 8: Three-dimensional modeling of the gap regions around the side chains of Trp and its analogues at position 187 at the convex side of the molecule (see Figure 1). The parameters (bond lengths and geometry) are taken from ref *39* (see also Scheme 1). Cavities are visualized graphically as blue solid surfaces and accompanied with the structure formulas of the mutant side chains as well as with the calculated exclusion volumes. The gap regions are viewed from the side site of the annexin structure, perpendicular to the plane of the indole ring (see Figure 1). (A) Native Trp187 occupies 73.7 Å^3 of the space (excluded volume) in its hydrophobic niche. (B) In the 5-FTrp annexin V there is no significant change in the excluded volume in comparison to the native counterpart, which is also obvious from visual inspection of the gaps. (C) 4-FTrp introduction into annexin V leads to an increase of the excluded volume for about $^1/_4$ (91.1 Å^3) in comparison to the native protein. Such increase is also evident by visual inspection of the drawn cavities (they are "thicker" than those of the wt protein form). (D) 6-FTrp-containing annexin V has also a significantly increased excluded volume in comparison to the native form and is similar to that of the 4-FTrp-substituted protein.

DISCUSSION

Spectral Properties of Tryptophan-like Noncanonical Amino Acids in Annexin V

Protein absorption and fluorescence are intrinsic properties based on the presence of aromatic amino acid side chains in the structure. Therefore, an expansion of the amino acid repertoire in the protein biosynthesis in vivo should allow for protein building with noncanonical aromatic amino acids that add special spectral properties to the structure of the protein variants. Such possibilities were already demonstrated, and it was shown that noncanonical analogues of tryptophan could serve as valuable intrinsic fluorophores (*7*). Our findings with annexin V are in line with the results and confirm the general usefulness of such spectroscopic probes built into proteins with noncanonical amino acids.

For example, annexin V containing the nonfluorescent 4-FTrp exhibits no fluorescence emission upon excitation at 280 nm, as shown in Figure 5. The emission maximum at 307 nm obtained upon excitation at 280 nm identifies unambiguously the contributions of Tyr residues to the emission spectrum. As the energy absorbed by 4-FTrp is not released as fluorescence, it has to be transferred to other residues. Indeed, Hott and Borkmann (*34*) demonstrated that 4-FTrp is significantly more photoactive than the parent Trp, with photolysis quantum yields 7 times larger than that of Trp. Additionally, 4-FTrp displays fluorescence at 77 K and 295 nm and a phosphorescence comparable to that of Trp at this temperature. On the other hand, both 5- and 6-FTrp-containing annexins V exhibit a red shift (13 and 16 nm) if compared to the wt protein (325 nm) and a significantly increased quantum yield upon excitation at 280 nm (Figure 5A). Excitation at 295 nm leads to a 3 nm red shift of 5-FTrp annexin V and about 6 nm of 6-FTrp annexin V. Explanation of these phenomena on the basis of previous studies of the strong influence of local environments on Trp fluorescence and its complex biophysical behavior (*7*, *35a*) would be too speculative. Detailed studies on simple model compounds produced by synthesis of peptides that contain such noncanonical Trp analogues could add the necessary information.

The Concept of "Atomic Mutations" for Protein Folding Studies

We performed our studies in the frame of the recently proposed concept of atomic mutations (*20*). It is expected to be a useful supplement to classical site-directed mutagenesis to attempt detailed microscopic descriptions of the energetics and mechanisms of folding transition processes. In fact, site-directed mutagenesis (codon manipulation) is performed at the level of recombinant DNA while "atomic" mutagenesis (codon reassignment) is carried out at the level of protein synthesis under a strong selective pressure (*1*). Atomic mutations are supposed to simplify the interpretation of experimental data, because unlike site-directed mutagenesis where usually several sets of interactions are affected, the altered protein properties arise solely from exchanges of single atoms. Thus, this approach offers rather novel possibilities for analyzing rationally distinct contributions of various local interactions to the protein stability and activity, such as hydrogen bonding and van der Waals, polar, and hydrophobic interactions, and to the folding cooperativity (*20*).

In the context of the present study, the term atomic mutation refers to the replacement of a single hydrogen atom by fluorine that brings only limited, crystallographically isomorphous changes in local geometries and alterations of

physicochemical properties. Our basic intention was to see to which extent stability as well as functional properties could be affected by the exchange of a single atom in a protein molecule composed of 320 residues, i.e., of 5328 atoms. The methodological drawback of this SPI method is that the atomic mutations occur in a *residue-specific* manner (*14*), meaning that each specific amino acid in the sequence is replaced. In this way it is difficult to recognize the single contribution of each substituted atom if more than one specific residue is present in the sequence. By combining the approach of atomic mutation with the classical site-directed mutagenesis techniques, such problems can be circumvented. Another possibility is to use a protein with only one target residue in the whole sequence. The presence of only one tryptophan residue in the amino acid sequence of annexin V (Trp187) proved to be of great advantage, offering the unique possibility of studying a single-atom exchange within the rest of the macromolecule.

In the frame of common-sense reasoning it is difficult to imagine that the exchange of a single atom, i.e., atomic mutation, at particular topological spots in the folded protein structure might produce any significant effects on protein structure, stability, and activity. Therefore, it is not surprising that until very recently the thermodynamic effects of atomic mutations at tryptophan residues on protein stability and folding cooperativity had not been investigated at all. The first report in this direction was performed on staphylococcal nuclease (*11*) where indeed effects of such subtle exchanges on the protein stability were found to be insignificant. Annexin V is similar to staphylococcal nuclease in terms of overall protein size, thermodynamic behavior, and estimated stability; e.g., GdmCl-induced unfolding gives similar values for both proteins (*20*), and both proteins contain a single Trp residue in their structure. A possible explanation for the markedly different results obtained with the two proteins upon tryptophan fluorination can be derived from a closer inspection of the X-ray structures. While Trp187 in annexin V is buried in a hydrophobic core, Trp140 of nuclease is relatively solvent accessible, particularly regarding positions 4, 5, and 6 of the indole ring. Upon unfolding, the indole moiety Trp187 in annexin V undergoes a transition from a hydrophobic to a water−solvent environment, while Trp140 of nuclease is already in contact with the bulk water. It is well-known that the main contribution to protein folding/unfolding energetics comes from buried residues that undergo transitions from the hydrophobic protein interior of the native state to the solvent environment of the unfolded state. Thus, solvation of Trp and of its noncanonical analogues during unfolding of annexin V might be the reason for the observed differences in the folding/unfolding energetics of the two proteins.

Large Global Effects with Minimal Local Changes

Far Beyond the Resolution of X-ray and NMR Protein Analyses. Changes in secondary (Figure 4) and tertiary structure (Figure 7) were minimal in the atomic mutants of annexin V, i.e., in the crystalline states all the mutants are isomorphous. It is now well documented that isomorphous protein structures often exhibit different thermodynamic behaviors in solution (*15, 20*). Until recently, there was "no information concerning the structural consequences of the substitution of fluorinated aromatic side chains in a macromolecular context" (*35b*). Indeed, it was reported for several proteins that single site-directed mutations can produce very large differences in the enthalpy, heat capacity, or free energies in denaturation experiments (*30*) without any significant change in the crystal structure. Since proteins are only marginally stable, all types of molecular interactions are important and even small interactions can contribute significantly to the stability (*36*). This is apparently the case in annexin V where the thermodynamic behavior of the crystallographically isomorphous mutants was found to differ significantly.

What Changes? Fluorination at different positions of the indole ring results in the following local effects: (i) increase in the covalent radii; i.e., the aromatic C−F bond is 0.3 *Å* longer than the aromatic C−H bond; (ii) inverted polarities and thus increased charge separation in the indole ring (Scheme 1); (iii) changed hydrogen bond acceptor ability; i.e., fluorine is a weak hydrogen bond acceptor; (iv) altered solubility as well as water ↔ organic solvent energy transfer.

Hydrophobicity. The hydrophobicity scales derived for Trp and its noncanonical counterparts from water/organic solvent distribution experiments are different and sometimes controversial. Ambiguities arise from the fact that there is no single reference phase that could serve as a general model for the interior of a globular protein. For example, Fauchere and Pliska (*37*) found Trp to be the most hydrophobic amino acid using 1-octanol as reference solvent for comparison with water in distribution experiments. On the other hand, Radzicka and Wolfenden (*38*) found by using cyclohexane that the side chain of Trp is about 25 times less hydrophobic than that of phenylalanine. Even distribution experiments with the same reference phase (1-octanol) for 5-FTrp and 6-FTrp performed by two different groups yielded contradictory results. Xu et al. (*39*) found 5-FTrp more hydrophobic than Trp, 6-FTrp, and 4-FTrp, while the measurements of Wong and Eftnik (*11*) indicated 6-FTrp as the most hydrophobic compound in this group.

Taking into account these data, it is hard to attribute without ambiguity any of the observed folding parameters to the hydrophobicity scale of tryptophan and its noncanonical analogues. In fact, if 5-FTrp is really the most hydrophobic amino acid among the analogues, this could account for the higher cooperativity and stability in the denaturation experiment since burial of more hydrophobic residues leads to more stable proteins (*40*). The lowest charge separation, *i.e.*, polarity, of 5-FTrp among the analogues also fits well into this picture. However, difficulties arise assuming higher hydrophobicities of 4-FTrp and 6-FTrp as determined by Wong and Eftnik (*11*) or deducible from the behavior of these amino acids in the amino acid analyses. If they are really more hydrophobic, why does their introduction into the annexin structure lead to lower estimated stabilities?

Indeed, there is a increasing evidence that burial of hydrophobic surface areas alone is insufficient to explain the observed changes brought by atomic mutations (*41*). Furthermore, the hydrophobic effect alone seems to be insufficient to account for the existence of a unique equilibrium structure in proteins since aggregates of oil, which form spontaneously in water, lack specific internal architecture (*42*). Obviously, satisfactory explanation requires including factors other than hydrophobicity alone to find possible reasons for such a behavior.

Local Geometry. Since X-ray analysis shows perfect isomorphism of the mutants with the native structure (Figure 7), subtle changes introduced with the Trp analogues are apparently suppressed or annihilated by strong crystal lattice contacts. However, a closer crystallographic inspection shows that Phe194 is in van der Waals contact with position C4 of Trp187. Thus, the lowered stability of the 4-FTrp atomic mutant could originate from repulsion of the negatively polarized fluorine atom that is pointing to the middle of the Phe side-chain ring. On the other hand, there is no steric hindrance for the fluorine atom at position 6 of the indole ring, thus raising again ambiguity to the attempts in explaining the lowered stability of the 6-FTrp mutant with local geometry changes.

Molecular Packing. It has been postulated that the "molecular packing, the efficient filling of the space, may be the most generally applicable factor that leads to the unique structures of most globular proteins" (*43*). Keeping this in mind, we have performed molecular modeling and calculation of the exclusion volumes, hoping to obtain more information about efficient packing of the tryptophan side chain. Indeed, our results allow speculating about tighter packing of wt and 5-FTrp annexin V and their similar stabilities (Figure 8A,B). Moreover, the fluorine atom in position 5 of the indole ring seems to fit well into the local geometry of the Trp187 environment, thus not causing any sterical repulsion. Conversely, the packing of 4-FTrp and 6-FTrp (Figure 8C,D) into the core seems to be by $^1/_4$ less tight, therefore indicating possible unfavorable electrostatic or even steric interactions. The near-UV CD profiles revealed also 6-FTrp annexin V as the most mobile mutant followed by 4-FTrp and 5-FTrp annexin V (Figure 4C). These findings correlate well with the thermodynamic stabilities (Table 2) and in part with the activity data.

van der Waals Interaction and Polarity. The best approach for understanding the modeling experiments is probably to assume that "making isosteric mutations does not mean 'no change' in van der Waals interactions, because two different shapes having the same volume can pack a cavity differently" (*44*). The van der Waals radius of fluorine is only 0.15 Å larger than that of hydrogen (*45*). In our pervious work on Met atomic mutations it was also concluded that "an increase in van der Waals radii and electronegativities may have strong impacts on the protein restricted internal architecture, i.e., packing, matching, and adjustment of the local surfaces, and consequently on the folding parameters" (*20*). As a consequence of the polarity change of the C−F bond the electron densities of the substituted carbon atoms are reduced, in the following order (expressed as net charge of the C atom): 4-FTrp > 6-FTrp > 5-FTrp (see Scheme 1). Furthermore, the electronic properties of the indole ring are complex (*35*). Thus, it might be possible that reorientation of solvent molecules for the fluorinated Trp residues may lead to different dipole moments which then can influence folding parameters.

By keeping all this in mind it is not surprising to find significant effects by single and local H → F replacements in a system composed of 5328 atoms. Moreover, fluorine as one of the most electronegative atoms might represent a good example to demonstrate how this particular physical property, i.e., the electronegativity, is integrated and modulated in a highly structured and hierarchically organized cooperative protein system which performs such sophisticated tasks in living cells such as voltage-gated channeling (*16*, *21*, *22*).

Bioactivity

In most cases substitution of canonical residues in proteins with noncanonical ones does not have any significant effect on the activity, presumably because the exchanged residues in these proteins do not play a functionally important role. Taking into account the special role of Trp187, annexin V provides an excellent model for studying effects on bioactivity. Upon membrane binding the tryptophan side chain flips out of its pocket and inserts partially into the membrane. 6-FTrp annexin V easy undergoes such transition since it has a 3 times higher efficiency for mediating calcium influx through the liposome membrane. Surprisingly, the 4-FTrp mutant, despite being as less tightly packed as the 6-FTrp mutant, shows only 32% activity, while the 5-FTrp mutant has about 50% of the wt protein activity. The absence of correlation between thermodynamic stability and activity can only be attributed to a different role of the polarities of the indole moiety in folding and bioactivity of annexin V. The different effect of the polarities in different contexts is well evidenced by comparing the results of the present study with the efficiency of fluorinated Trp analogues in competing with Trp as substrates of the tryptophanyl-tRNA synthetase (*39*). In these classical steady-state enzyme kinetic experiments the activities followed the order Trp > 4-FTrp > 6-FTrp > 5-FTrp (*39*). Thus, it is obvious that more work is required to see whether general rules exist that can plausibly describe possible effects of the presence of noncanonical amino acids in various proteins in terms of their function and stability.

Integration and Modulation of New Physicochemical Properties in the Protein Structure

A quantitative understanding of the noncovalent forces that define specific, but marginally stable native protein structures is one of the most important goals of many laboratories dealing with the protein folding problem. Unfortunately, satisfactory explanations of the energetic effects caused by single site mutations are seldom, since it is difficult to assess "over what range of distance from the site of the mutation significant structural changes are propagated" (*47*). It is anticipated that introduction of the noncanonical amino acids into the proteins allows for subtle replacement of "natural" by "nonnatural" making in this way a fine tool to study nonbonded interactions (*1*). Moreover, many of the atoms in this context are "xenoatoms", e.g., tellurium, selenium, or fluorine usually not found in natural proteins, and thus insert new properties into the native structure such as increased or decreased polarity, electronegativity, and electrovalent and coordination spheres. They are offering the unique possibility of monitoring how these properties are integrated, propagated, or even modulated into the cooperatively folded protein structure.

It has not escaped to our attention that physicochemical properties introduced by such atomic mutations are differently (positively or negatively) propagated (amplified) through the cooperative integration process during folding of the protein, resulting in crystallographically isomorphous but thermodynamically different structures. In other words, these properties (hydrophobicity, polarity) are synergistically

modulated in the protein structure, explaining in this way rather large global effects in the whole macromolecule as a result of rather minimal local changes. In fact, from theoretical analysis it was proposed that the change in total energy content of a system like one uniquely folded protein associated with altering a specific interaction will depend on the correlation between that interaction and all other interactions in the system (*46*).

ACKNOWLEDGMENT

We thank Andreas Bergner for help in modeling calculations and Andreas Hofmann for channel activity and FURA-2 measurements of annexin V. We acknowledge Anja Dorowski and Heike Krupka for help in the crystallographic calculations. We are particularly indebted to Mrs. Elisabeth Weyher and Mrs. Waltraud Wenger for their excellent technical assistance.

REFERENCES

1. Budisa, N., Minks, C., Alefelder, S., Wenger, W., Dong, F., Moroder, L., and Huber, R. (1999) *FASEB J. 13*, 41−51.
2. Steward, L. E., Collins, C. S., Gilmore, M. A., Carlson, J. E., Ross, J. B. A., and Chamberlin, A. R. (1997) *J. Am. Chem. Soc. 119*, 6−11.
3. Royer, C. A. (1995) *Methods Mol. Biol. 40*, 65−89.
4. Pardee, A. B., and Prestidge, L. S. (1958) *Biochim. Biophys. Acta 27*, 330−344.
5. Brawerman, G., and Ycas, M. (1957) *Arch. Biochem. Biophys. 68*, 112−117.
6. Schlesinger, S. (1968) *J. Biol. Chem. 243*, 3877−83.
7. Hogue, C. W., Doublie, S., Xue, H., Wong, J. T., Carter, C. W. Jr., and Szabo, A. G. (1996) *J. Mol. Biol. 260*, 446−66.
8. Ross, J. B., Szabo, A. G., and Hogue, C. W. (1997) *Methods Enzymol. 278*, 151−190.
9. Pratt, E. A., and Ho, C., (1975) *Biochemistry 14*, 3035−3039.
10. Bronskill, P. M., and Wong, J. T. (1988) *Biochem. J. 249*, 305−308.
11. Wong, C. Y., and Eftink, M. R. (1998) *Biochemistry 37*, 8938−8946.
12. Soumillion, P., Jespers, L., Vervoort, J., and Fastrez, J. (1995) *Protein Eng. 8*, 451−456.
13. Huber, R., Romisch, J., and Paques, E. (1990) *EMBO J. 9*, 3867−3974.
14. Budisa, N., Steipe, B., Demange, P., Eckerskorn, C., Kellermann, J., and Huber, R. (1995) *Eur. J. Biochem. 230*, 788−796.
15. Budisa, N., Minks, C., Medrano, F. J., Lutz, J., Huber, R., and Moroder, L. (1998) *Proc. Natl. Acad. Sci. U.S.A. 95*, 455−459.
16. Benz, J., and Hofmann, A., (1997) *Biol. Chem. 378*, 177−83.
17. Sopkova, J., Gallay, J., Vincent, M., Pancoska, P., and Lewit-Bentley, A. (1994) *Biochemistry 33*, 4490−4499.
18. Tabor, S., and Richardson, C. (1985) *Proc. Natl. Acad. Sci. U.S.A. 82*, 1074−1078.
19. Budisa, N., Karnbrock, W., Steinbacher, S., Humm, A., Prade, L., Neuefeind, T., Moroder, L., and Huber, R. (1997) *J. Mol. Biol. 270*, 616−623.
20. Budisa, N., Huber, R., Golbik, R., Minks, C., Weyher, E., and Moroder, L (1998) *Eur. J. Biochem. 253*, 1−9.
21. Berendes, R., Burger, R., Voges, D., Demange, P., and Huber, R. (1993) *FEBS J. 317*, 131−134.
22. Hofmann, A., Benz, J., Liemann, S., and Huber, R. (1997) *Biochim. Biophys. Acta. 1330*, 254−264.
23. Huber, R., Berendes, R., Burger, A., Schneider, M., Karshnikov, A., Luecke, H., Romisch, J., and Paques, E. (1992) *J. Mol. Biol. 223*, 683−704.
24. Leslie, A. G. W. (1991) Molecular data processing, in *Crystallographic computing 5: From Chemistry to Biology* (Moras, D., Podjarny, A. D., and Thierry, J. C., Eds.) pp 50−61, Oxford University Press, Oxford.
25. Otwinowski, Z., and Minor, W. (1997) *Methods Enzymol. 276*, 307−326.
26. Collaborative Computational Project, number 4. (1994) *Acta Crystallogr. D50*, 760−763.
27. Brünger, A. (1992) *X-PLOR Version 3.1, A system for X-ray Crystallography and NMR*, Yale University Press, New Haven, CT.
28. Roussel, A., and Cambilleau, C. (1992) *TURBO−FRODO*, Biographics, LCCMB, Marseille, France.
29. Laskowski, R. A. (1995) *J. Mol. Graphics 13*, 323−330.
30. Carra, J. H., and Privalov, P. L. (1996) *FASEB J. 10*, 67−74.
31. Sopkova, J., Vincent, M., Takahashi, M., Lewit-Bentley, A., and Gallay, J. (1998) *Biochemistry 37*, 11963−11971.
32. Budisa, N. (1997) Ph.D. Thesis, Technische Universität, München.
33. Meers, P., and Mealy, T. R. (1993) *Biochemistry 32*, 11711−11721.
34. Hott, J. L., and Borkmann, R. F., (1989) *Biochem. J. 264*, 297−299.
35. (a) Hudson, B. S., Harris, D. L., Ludescher, R. D., Ruggiero, A., Cooney-Freed, A., and Cavalier, S. A. (1986) in *Applications of Fluorescence in the Biomedical Sciences*, pp 159−202, Alan R. Liss, Inc., New York. (b) Xiao, G., Parsons, J. F., Armstrong, R. N., and Gilliland, G. L. (1997) *J. Am. Chem. Soc. 119*, 9325−9326.
36. Dill, K. A. (1990) *Biochemistry 29*, 7133−7155.
37. Fauchere, J. L., and Pliksa, V. E. (1983) *Eur. J. Med. Chem. 18*, 369−375.
38. Radzicka, A., and Wolfenden, R. (1988) *Biochemistry 27*, 1644−1670.
39. Xu, Z. J., Love, M. L., Ma, L. Y., Blum, M., Bronskill, P. M., Bernstein, J., Grey, A. A., Hofmann, T., Camerman, N., and Wong, J. T. (1989) *J. Biol. Chem. 264*, 4304−4311.
40. Spolar, R. S., Livingstone, J. R., and Record, M. T., Jr. (1992) *Biochemistry 31*, 3947−3955.
41. Thompson, J., Ratnaparkhi, G. S., Vardarajan, R., Sturtevant, J. M., and Richards, F. M. (1994) *Biochemistry 33*, 8587−8593.
42. Rose, G. D., and Wolfenden, R. (1993) *Annu. Rev. Biophys. Biomol. Struct. 22*, 381−415.
43. Richards, F. M. (1997) *Cell. Mol. Life Sci. 53*, 790−802.
44. Dill, K. A., and Shortle, D. (1991) *Annu. Rev. Biochem. 60*, 795−825.
45. Brooks, B., and Benisek, W. F. (1994) *Biochemistry 33*, 2682−2687.
46. Mark, A. E., and van Gunsteren, W. F. (1994) *J. Mol. Biol. 240*, 167−176.
47. Shortle, D. (1996) *FASEB J. 10*, 75−83.
48. Kraulis, P. J. (1991) *J. Appl. Crystallogr. 24*, 946−950.

BI990580G